Computation of Water and Air Flow with Submerged Hydrofoil by Interface Capturing Method

Seung-Hyun Kwag*
School of Mechanical Engineering, Halla University

Free-surface flows with an arbitrary deformation, induced by a submerged hydrofoil, are simulated numerically, considering two-fluid flows of both water and air. The computation is performed by a finite volume method using unstructured meshes and an interface capturing scheme to determine the shape of the free surface. The method uses control volumes with an arbitrary number of faces and allows cellwise local mesh refinement. The integration in space is of second order, based on midpoint rule integration and linear interpolation. The method is fully implicit and uses quadratic interpolation in time through three time levels. The linear equations are solved by conjugate gradient type solvers, and the non-linearity of equations is accounted for through Picard iterations. The solution method is of pressure-correction type and solves sequentially the linearized momentum equations, the continuity equation, the conservation equation of one species, and the equations for two turbulence quantities. Finally, a comparison is quantitatively made at the same speed between the computation and experiment in which the grid sensitivity is numerically checked.

Key Words : Two Fluid Flows, Finite Volume Method, Submerged Hydrofoil, Free Surface, Viscous Flow Simulation, Interface Capturing Scheme

Nomenclature

ρ : Fluid density
n : Unit normal vector outwards
V : Control volume
θ : Angle normal to the interface
v : Fluid velocity vector
v_b : Velocity of the control surface
p : Pressure
b_i : Body force
μ : Dynamic viscosity of fluid
τ_{ij} : Effective stress
c : Void fraction of liquid

1. Introduction

Computation of flows, including the deformation of the free surface, is one of the big challenges in fluid mechanics. Many methods (Farmer et al., 1994, Muzaferiza et al., 1997) of this kind have been developed and successfully applied to flows. However, if the body form is complicated, these methods are difficult to use because the grid has to be adapted both to the free surface and body shape: the grid may deform too much in this process and a re-gridding may become necessary. When the body form is relatively simple, the interface tracking approach is convenient in which only the water flow is computed and the grid moves to adapt to the free surface.

Another difficulty in handling interface tracking methods is the breaking, overturning, or wave splashing. In many cases, it is important to compute the flows of both liquid and gas simultaneously, especially when the gas is enclosed by liquid and bouyancy effects become important. For this reason, interface capturing methods have to be used. The MAC (Harlow et al., 1965) and VOF (Hirt et al., 1981) methods are of this kind, although the air flow is not actually computed.

* **E-mail** : shkwag@hit.halla.ac.kr
TEL : +82-371-760-1233 ; **FAX** : +82-371-762-6705
School of Mechanical Engineering, Halla University, 66 Heungup, Wonju 220-712, Korea. (Manuscript **Received** March 24, 1999; **Revised** April 26, 2000)

Recently the density function method (Kawamura et al., 1994) and two-fluid models (Ubbink, 1997, Muzaferija et al., 1998) have been developed. The last is used here to demonstrate its applicability to the submerged hydrofoil flows. It is based on the finite volume (FV) approach and uses unstructured grids with arbitrary polyhedral control volumes (CVs). Both air and water are considered as a single fluid with variable properties. An additional transport equation for the void fraction of liquid is solved to determine the interface between the two fluids. A special discretized scheme for convective fluxes in the void fraction equation is used to ensure the sharpness of the interface. The computational results are presented for the viscous flows induced by NACA 0012 hydrofoil.

2. Basic Euations and Numerical Strategy

Basic equations for mass, momentum and volume fraction are expressed in their integral form, which for an arbitrary, moving control volume can be written as,

$$\frac{d}{dt}\int_V \rho dV+\int_S \rho(\boldsymbol{v}-\boldsymbol{v}_b)\cdot \boldsymbol{n}dS=0 \quad (1)$$

$$\frac{d}{dt}\int_V \rho u_i dV+\int_S \rho u_i(\boldsymbol{v}-\boldsymbol{v}_b)\cdot ndS = \int_S(\tau_{ij}-pi_i)\cdot ndS+\int_V \rho b_i dV \quad (2)$$

$$\frac{d}{dt}\int_V c dV+\int_S c(\boldsymbol{v}-\boldsymbol{v}_b)\cdot \boldsymbol{n}dS=0 \quad (3)$$

where ρ is the fluid density, V is the control volume (CV) bounded by a closed surface S, $\boldsymbol{v}$ is the fluid velocity vector whose Cartesian components are u_i, $\mathrm{v_b}$ is the velocity of the control surface, t is the time, p is the pressure, c is the void fraction of liquid, b_i is the body force in the direction of the Cartesian coordinate x_i, $\boldsymbol{n}$ is the unit normal to S and directed outwards, and τ_{ij} are the components of the viscous stress tensor defined for Newtonian incompressible fluids considered here as,

$$\tau_{ij}=\mu\left(\frac{\partial u_i}{\partial x_j}+\frac{\partial u_j}{\partial x_i}\right) \quad (4)$$

with μ being the dynamic viscosity of the fluid.

When the control volume moves, the so called *space conservation law* (SCL) has also to be satisfied; it is expressed by the following relation between the rate of change of CV and its surface velocity:

$$\frac{d}{dt}\int_V dV-\int_S \boldsymbol{v}_b\cdot \boldsymbol{n}dS=0 \quad (5)$$

These equations are applied to each CV and discretized in order to obtain one algebraic equation per CV; each equation involves the unknown from the CV-center (where all knowns are stored) and from a certain number of neighboring CVs. Here second-order approximations (linear interpolation, central differences, and midpoint rule integration) are used to evaluate the integrals in space and time. The method is fully implicit, i. e., the spatial integrals are evaluated at the new time level, while the old values appear only in the approximation of the time derivative (linear or quadratic backward scheme). For more details on discretization methods, see (Ubbink, 1997, Muzaferiza et al., 1998)

Both fluids are treated as single effective fluids whose properties vary in space according to the volume fraction of each phase, i. e.,

$$\rho=\rho_1 c+\rho_2(1-c),\ \mu=\mu_1 c+\mu_2(1-c) \quad (6)$$

where subscripts 1 and 2 denote the two fluids (liquid and gas). If one CV is partially filled with one fluid and partially with the other (i. e., $0\leq c\leq 1$), it is assumed that both fluids have the same velocity and pressure. The free surface does not represent a boundary and no boundary conditions need to be prescribed on it. The critical issue in this type of methods is the discretization of convective term in Eq. (3). Since c must obey the bounds $0\leq c\leq 1$, one has to ensure that the scheme does not generate overshoots or undershoots, but it should also keep the interface as sharp as possible, since the fluids should not mix. As noted above, the solution domain extends over both fluids, and all the conservation equations are solved in the whole domain. At the initial time step, the discretization of c is prescribed, defining the initial location of liquid and the shape of the free surface. Equation (3) is for the void fraction of one phase, c. The grid extends over both liquid

and gas; one sets c=1 in CVs filled by water and c=0 in CVs filled by air. The change of c is governed by the transfort Eq. (3). The only scheme which unconditionally satisfies the boundedness criterion is the first order upwind scheme: however it can not be used due to excessive numerical diffusion, which smears the interface so badly that the two fluids mix over a wide region.

On the other hand, any of the higher order schemes tends to produce over-and undershoot in the vicinity of discontinuities. One can resort total variation capturing (TVD) and essentially non -oscillating (ENO) schemes. However, the interface capturing in the free surface flows has some special features which need to be considered. One comes from the fact that the convective flux out of one CV must not transport more of one fluid than is available in the donor cell. During the computation of the cell-face values of c, the orientation and the local Courant number should be taken into account of.

The sharpness of the interface without over- and undershoots can be achieved by limiting the approximation of the cell-face value to lie in the shaded area of the so called *normalized variable diagram* (*NVD*) (Leonard, 1997) shown in Fig. 1. The local normalized variable c in the vicinity of the cell-center C is defined

$$\tilde{c}(\boldsymbol{r})=\frac{c(r)-c_U}{c_D-c_U} \tag{7}$$

where subscripts 'U' and 'D' denote nodes upstream and downstream of the cell-center C, and $\boldsymbol{r}$ is the position vector. Should the cell-center value $\tilde{c}_C$ turn out to be smaller than zero or larger than unity, this means that the profile of c is not monotonic and the numerical diffusion is needed to get rid of oscillations; first-order upwind scheme is then used to compute the cell-face values. For values of $\tilde{c}_C$ between zero and unity, one can choose any dependency from the shaded region of the NVD-diagram in Fig. 1. The particular choice selected here is indicated in Fig. 1 as HRIC (high resolution interface capturing) scheme; it is a combination of a linear upwind and a downwind scheme. The cell-face value resulting from the HRIC-scheme is further corrected according to the local Courant number and the angle between the free surface and the cell face. The aim of these corrections is to avoid instability problems at high Courant numbers (by adding more of the upwind scheme) and the occurrence of steps in the free surface. The following definitions are used.

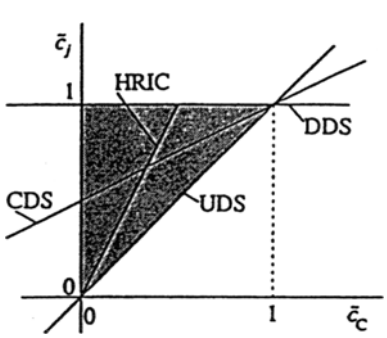

Fig. 1 Normalized variables diagram (CDS: Central Diff. Scheme, DDS: Downward, UDS: Upwind, HRIC: High Resolution Interface Capturing)

$$C_o=\frac{\boldsymbol{v}\cdot\boldsymbol{n}S_j\Delta t}{\Delta V_c} \tag{8}$$

$$\tilde{c}_j=\begin{cases}\tilde{c}_C & \text{if } \tilde{c}_C<0.0\\ 2\tilde{c}_C & \text{if } 0.0\le\tilde{c}_C\le0.5\\ 1 & \text{if } 0.5\le\tilde{c}_C\le1.0\\ \tilde{c}_C & \text{if } 1.0\le\tilde{c}_C\end{cases} \tag{9}$$

$$\tilde{c}^*{}_j=\begin{cases}\tilde{c}_j & \text{if } c_o<0.3\\ \tilde{c}_C+(\tilde{c}_j-\tilde{c}_C)\dfrac{0.7-C_o}{0.7-0.3} & \text{if } 0.3\le c_o\le0.7\\ \tilde{c}_C & \text{if } 0.7\le c_o\end{cases} \tag{10}$$

$$\tilde{c}_j{}^{**}=\tilde{c}_j{}^*\sqrt{\cos\theta}+\tilde{c}_C(1-\sqrt{\cos\theta}) \tag{11}$$

where θ represents the angle between the normal to the interface (represented by the gradient vector of c) and the normal to the cell face. Finally, the cell-face value of c is computed according to Eq. (7) as

$$c_j=\tilde{c}_j{}^{**}(c_D-c_U)+c_U \tag{12}$$

3. Application and Discussion

In order to demonstrate the suitability of the solution method described above, results of computations are presented. The aim of the present example is to show that the interface capturing method can treat the extreme deformation of the

free surface including its overturning and air enclosures.

The submerged hydrofoil is used for computation whose angle of attack is 30°; section shape is NACA0012, Froude number is 0.567, Reynolds number is 10^3 and 1.776×10^6, and turbulence model is of the k-ε RNG type. The number of cell is 13540, time increment is 0.0005 in a nondimensional unit, and the reference pressure is 10^5 Pa. Here the nondimensional time t means the ratio of the moved distance to the length of the body. In case t=1.0, the moved distance equals to exactly the length of the hydrofoil.

The minimum value of y^+ is 5 and maximum 410. The calculated total drag is 25.60 N and total lift force is 202.90 N. The computational conditions for the laminar and turbulent flows are as follows.

-Linear algebraic equation solver: Incomplete Cholesky preconditioned conjugate gradient
-Gradient calculation: Least square fit
-Free surface: Front capturing model
-Surface tension coeff. : 7.4×10^{-2} N/m
-Piezometric pressure, no slip (wall)
external: zero gradient
-Solution control

	momentum	mass	turbulence
relaxation factor	0.9	0.2	0.9
blending factor	0.9	1.0	1.0
solver tolerance	0.1	0.05	1.0
iteration number	50	500	50

Figure 2 shows the coordinate system for computation in which α is the angle of attack and d submergence depth. Figure 3 shows the computed results of the two fluids including free-surface for the laminar flows. Both liquid and gas flows are computed. This is important when gas is trapped in liquid or when gas flows with a high velocity. Since the grid does not have to be adapted to the shape of the free surface, problems with grid adaptations are avoided. The unstructured grid can be seen in Fig. 3(a) where the finer grid is used in some part of the free-surface and behind the trailing edge mostly influenced by the hydrofoil. The volume fraction is simulated along the time from t=3.0 to 5.0. The breaking or overturning is well captured without any numerical difficulties. This is one of the advantages of the interface capturing method. The overall pressure contour is seen in Fig. 3(c) with a perspective view around the leading edge. The velocity vectors are simulated for two fluids: air and water region. In the computation of laminar flows, the free surface may deform in an arbitrary manner; the present interface capturing method can simulate the shape of the free surface with the surface tension.

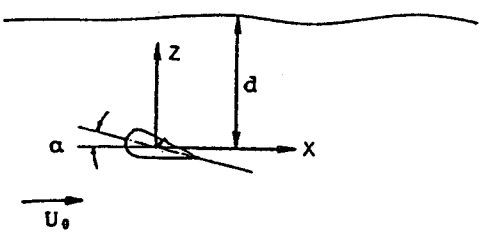

Fig. 2 Coordinate system for computation

Figure 4 shows the computed results for the turbulent flows. As seen in Fig. 4(a), the present method predicts well the extreme deformation of the free-surface. The pressure, velocity and volume fraction are seen in Fig. 4(b), (c) and (d), respectively. In the numerical solution procedure, the outer iteration of momentum and pressure correction equations are performed first in which the value of the eddy viscosity is based on the value of k and ε at the end of the preceding iteration. After this has been completed, an outer iteration of the turbulent kinetic energy and dissipation equations is made. Since these equations are highly nonlinear, they have to be linearized prior to iteration. After completing an iteration of the turbulence model equations, it is necessary to recalculate the eddy viscosity and start a new outer iteration. Figure 4(e) shows the contour of the kinetic energy obtained by the turbulence model of the k-ε RNG type.

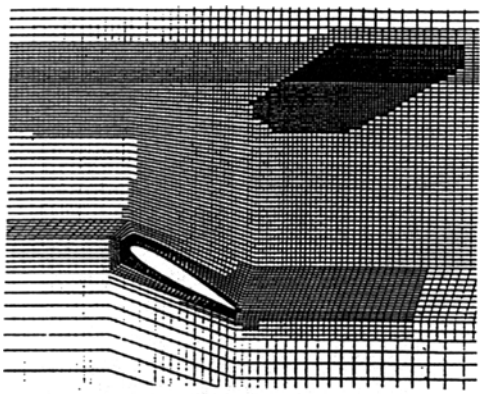

Fig. 3(a) Unstructured grid view (laminar)

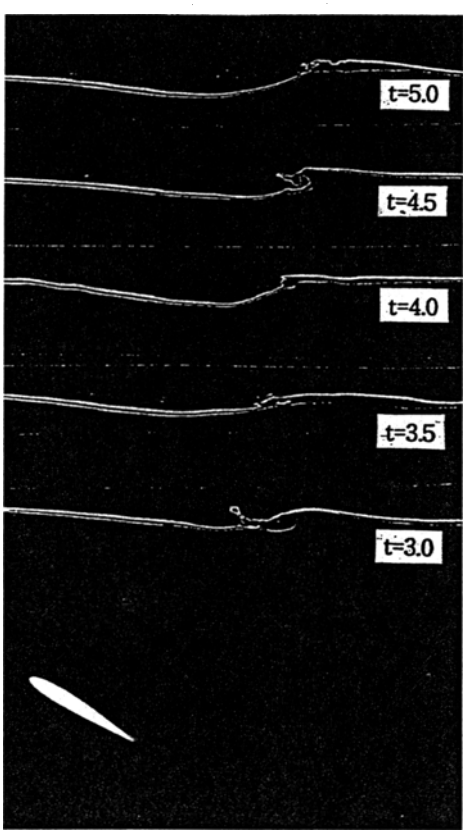

Fig. 3(b) Volume fraction (laminar)

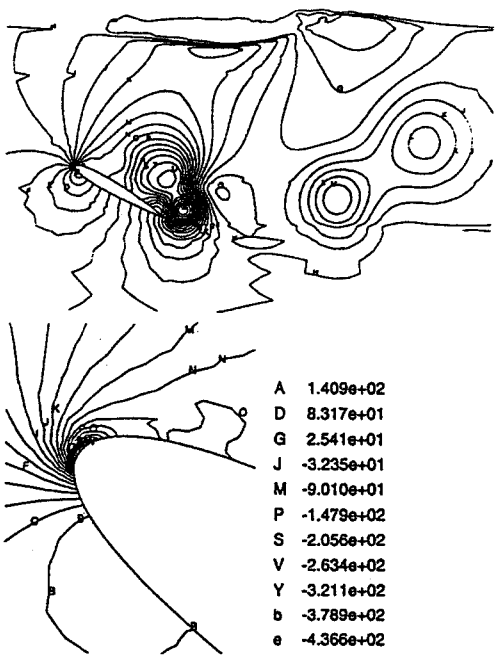

Fig. 3(c) Pressure distribution (laminar)

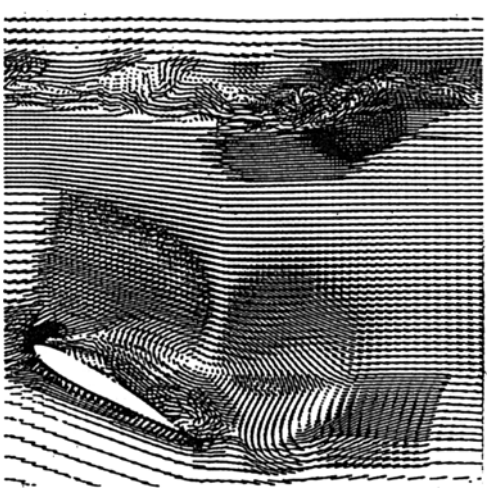

Fig. 3(d) Velocity vectors (laminar)

Figures 5 and 6 show the comparison of solutions obtained by using the interface-tracking and capturing method, respectively. This was also found in other applications (Muzaferija et al., 1998). The computations were performed using four systematically refined grids with 1004, 4016, 16064 and 64256 CVs respectively, in order to assess the discretization errors. Figure 5 shows the wave profiles computed on the four grids using the interface-tracking method, compared with experimental data (Duncan, 1983). The difference between solutions on subsequent grids is reducing with grid refinement, indicating convergence towards a grid-independent solution. The comparison with the experimental data shows that the grid-independent numerical solution will still

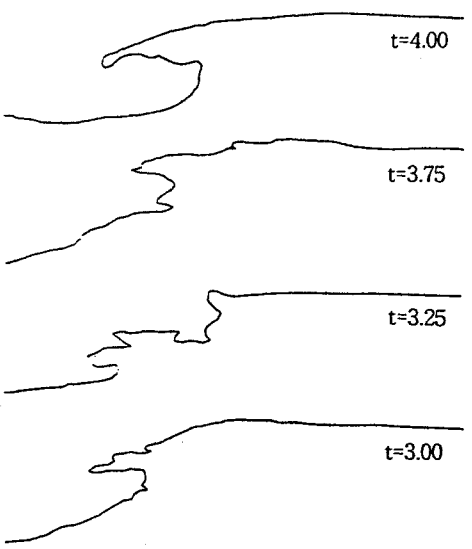

Fig. 4(a) Free surface height (turbulent)

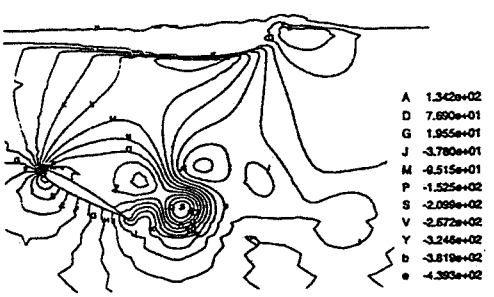

Fig. 4(b) Pressure distribution (turbulent)

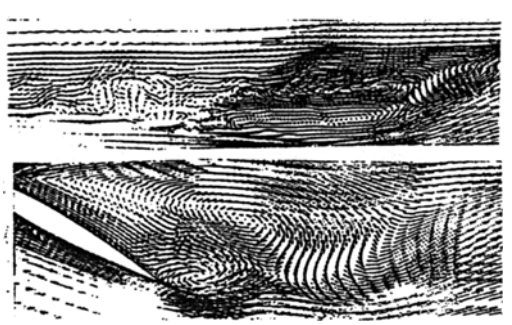

Fig. 4(c) Velocity vectors (turbulent) (above: near free-surface)

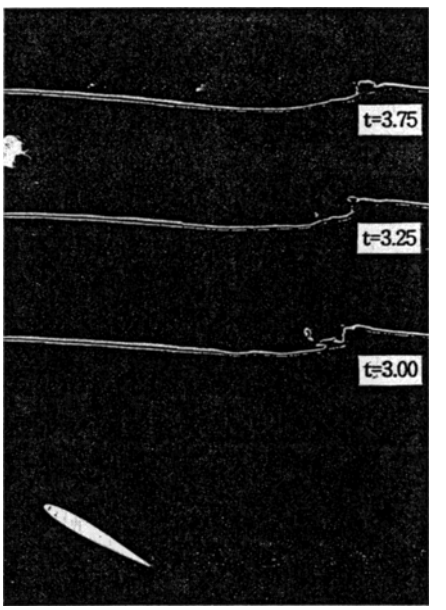

Fig. 4(d) Volume fraction (turbulent)

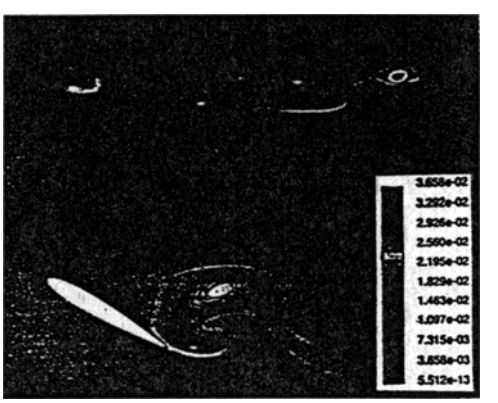

Fig. 4(e) Kinetic energy contour

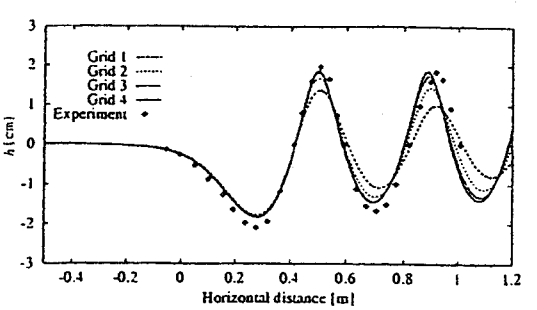

Fig. 5 Free-surface profile in the flow around a subsequent NACA0012 hydrofoil computed by interface-tracking method on the four systematically refined grids, compared to experimental data of Duncan (1983)

appreciably differ from experimental observation. While the maximum elevation appears to be almost the same in the experiment and in the simulation, the trough depths and the wavelength are smaller in the simulation than in the experi-

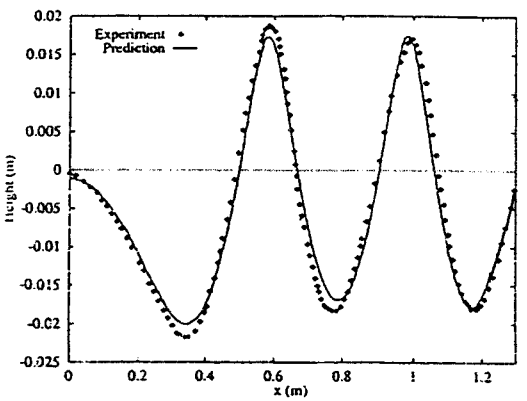

Fig. 6 Free-surface profile in the flow around NACA0012 hydrofoil computed by the interface-capturing method on the third grid from Fig. 5 (16064 CV plus an additional 2000 CVs in the air region above the free surface), compared to experimental data of Duncan (1983)

ment.

The computation conditions are as below; submerged hydrofoil of NACA0012, chord length (l_c) 203mm, maximum thickness 25.4 mm, 61 mm located behind the nose, angle of attack 5°, towing velocity 0.8 m/sec and Froude number 0.567. Figure 6 shows the free-surface profile in the flow by the interface capturing method on the third grid from Fig. 5, compared to experimental data of Duncan (1983).

4. Concluding Remarks

The interface capturing method allows the computation of flows around bodies of arbitrary complexity, since the grid need not to be adapted to the shape of the free surface. The interface capturing method presented here is applicable to flows with an arbitrary deformation of the free surface. It can capture free-surface nonlinear flows induced by a submerged hydrofoil, including breaking waves when the grid is locally refined. The results are comparable to those from the interface tracking methods with moving grids. Besides, the solution method allows the use of arbitrary control volumes and cellwise local mesh refinement, which is very useful for the complex flows. Finally, a comparison is made between the computation and experiment in which the grid sensitivity is numerically checked.

References

Duncan, J. H., 1983, "The Breaking and Non-Breaking Wave Resistance of a Two-Dimensional Hydrofoil," *J. Fluid Mech.*, Vol. 126, pp. 507~520.

Farmer, J., Martinelli, L. and Jameson, A., 1994, "Fast Multigrid Method for Solving Incompressible Hydrodynamic Problems with Free Surfaces," *AIAA J.*, Vol. 32, pp. 1175~1182.

Harlow, F. H. and Welch, J. E., 1965, "Numerical Calculation of Time Dependent Viscous Incompressible Flow with Free Surface," *Phys. Fluids*, Vol. 8, pp. 2182~2189.

Hirt, C. W. and Nicholls, B. D., 1981, "Volume of Fluid (VOF) Method for Dynamics of Free Boundaries," *J. Comput. Phys.*, Vol. 39, pp. 201~221.

Kawamura, T. and Miyata, H. 1994, "Simulation of Nonlinear Ship Flows by Density Function Method," *J. Soc., Naval Arch., Japan*, Vol. 176, pp. 1~10.

Leonard, B. P., 1997, "Bounded Higher Order Upwind Multi Dimensional Finite Volume Convection Diffusion Algolithms," in W. J. Minkowycz, E. M. Sparrow, *Advances in Numerical Heat Transfer*, Chap. 1, Taylor and Francis, New York, pp. 1~57.

Lin, J. C. and Rockwell, D., 1995, "Evolution of a Quasi Steady Breaking Wave," *J. Fluid Mech.*, Vol. 302, pp. 29~44.

Muzaferija, S. and Peric, M., 1998, "Computation of Free Surface Flows Using Interface Tracking and Capturing Methods," Chap. 3, in O. Mahrenholtz and M. Markiewicz, *Nonlinear Water Wave Interaction, Computational Mechanics Publications, Southampton.*

Muzaferija, S. and Peric, M., 1997, "Computation of Free Surface Flows Using Finite Volume Method and Moving Grids," *Numer. Heat Transfer*, Part B, Vol 32, pp. 369~384.

Ubbink, O., 1997, "Numerical Prediction of Two Fluid Systems with Sharp Interfaces," Ph. D. Thesis, Univ of London.